



WETFEET

D4.4 - Global analysis of the selected PTO for the Symphony

DATE: June 2018

PROJECT COORDINATOR:
WavEC Offshore Renewables

GRANT AGREEMENT NR: 641334
PROJECT: WETFEET



The WETFEET – Wave Energy Transition to Future by Evolution of Engineering and Technology project has received funding from the European Union's Horizon 2020 programme under grant agreement No 641334.

Report with global analysis of the selected PTO for the Symphony based on the bench tests and further engineering considerations			
Project	WETFEET – Wave Energy Transition to Future by Evolution of Engineering and Technology		
WP No.	4	WP Title	Electro-mechanic PTO Breakthrough
Deliverable No.	4.4		
Nature (R: <i>Report</i> , P: <i>Prototype</i> , O: <i>Other</i>)	R		
Dissemination level (PU, PP, RE, CO)	PU		
Lead beneficiary:	Teamwork Technology		
Contributing partners	Teamwork Technology		
Authors List:	Djurre Wikkerink; Roelof Schuitema; Fred Gardner		
Quality reviewer			
Status (F: final; D: draft; RD: revised draft):	F		
Due Delivery Date:	31/10/2017		
Actual Delivery Date:	29/06/2018		

Version no.	Dates and comments
1	First Draft
2	20-04-2018 Revised Draft Djurre Wikkerink
3	14-06-2018 final version
4	
5	

Table of Contents

EXECUTIVE SUMMARY	7
1. Introduction to Symphony.....	9
1.1 Operating Principle	9
1.2 The Generator.....	13
1.3 The end buffers.....	14
1.4 Time-Domain Model	15
2. Description of the PTO	18
2.1 Theoretical Efficiency.....	19
2.1.1 Slip losses.....	20
2.2.2 Friction Loss	24
2.1.4 Overall Evaluation.....	25
2.2 PTO conversion efficiency in realistic sea state conditions	26
2.3 Turbine Testing	29
2.3.1 Theoretical Loss Components	29
2.3.2 Test Setup and Instrumentation.....	30
2.3.4 Test Plan.....	31
3. Conclusions	32
BIBLIOGRAPHY	32

Table of figures

Figure 1: Different parts of the Symphony	9
Figure 2: Operating principle of the Symphony	9
Figure 3: Turbine venturi stretched.....	10
Figure 4: Turbine venturi.....	10
Figure 5: Turbine cross section	11
Figure 6: Operating principle PTO	12
Figure 7: The PTO of the Symphony.....	13
Figure 8: Schematic representation of the time-domain model	16
Figure 9: Cross section of the turbine.....	18
Figure 10: In and outlet diffusers	18
Figure 11: Losses within the gaps	19
Figure 12: Different leak ways within the turbine	20
Figure 13: Velocity profile of leak way 1	21
Figure 14: Top view runners	23
Figure 15: Theoretical efficiency of the turbine	25

Table of tables

Table 1: DIFFERENT LOSS COMPONENTS.....	30
-----------------------------------------	----

LIST OF ACCRONYMS

PTO	Power Take-Off
WEC	Wave Energy Converter
IGBT	Insulated-Gate Bipolar Transistor
PMSG	Permanent Magnet Synchronous Generator

EXECUTIVE SUMMARY

This report presents Deliverable 4.4 of the WETFEET H2020 project. The Deliverable describes the global analysis of the selected PTO for the Symphony WEC. It contains the engineering considerations, working principle and focuses on the efficiency of the turbine. In the initial setup, the PTO bench test results were part of the report and analysis. Some drawbacks and delays in the final assembly of the physical PTO prototype, caused that the bench test results could not be included in this deliverable. (see Deliverable D4.2).

During the early stages of the WETFEET project, the Symphony PTO was selected. The water turbine principle is chosen in favor of a spindle solution. Especially engineering considerations related to side way forces and the loads on the bearings was the main reason not to choose the spindle. Also the spindle construction was much less suitable for scaling up. (see Deliverable D2.2 chapter 3.5)

The water turbine in combination with the structural membrane are the main and innovative component in the Symphony WEC. In steps:

- a) waves push the Symphony floater downwards. (under a wave top)
- b) During the downward stroke, the membrane is pushed in a smaller gap than in its upper position.
- c) This results in a smaller membrane volume.
- d) The membrane contains water, the working fluid, which is pushed through the water turbine.
- e) The water turbine drives the electrical generator.
- f) The internal water flow is pushed in an air tank, building up an air pressure.
- g) The air pressure, an air spring, pushes back the water flow and the floater head (under a wave trough)

This sequence of operation, results effectively in a bi directional water flow through the turbine. The turbine spins up to a maximum of 350 rpm and slows down to 0, than it speeds up in the opposite direction.

This bi-directional and non constant rotational speed is delivered to the generator directly connected at the same shaft to produce electricity.

The water turbine is designed in such a way the flow passes as smoothly as possible. The inlet and outlet are optimized for the wave operation. The water turbine is an adjusted version of a displacement pump. The main adjustment is the layout of the rotors to ensure an as constant possible water flow to minimize turbulence and as such optimize the efficiency.

The efficiency of the PTO is calculated in several steps to include all contributions to energy losses in the system. The efficiency is expressed in an efficiency curve as function of the power and rotational speed.

For the whole Symphony device a time domain model is available to simulate the full system. The forces, velocities and energy conversations in the Symphony device are calculated as function of the incoming waves.

The turbine efficiency curve is added to the time domain model. For a complete series of sea states the resulting PTO efficiency could be calculated. So from the smallest cut in sea state ($T_e=4,5s$; $H_s=0,75m$) to the maximum operational sea state ($T_e=14,5s$; $H_s=4,5m$) the efficiency from the incoming wave to the electrical output is found.

The conversion from the hydraulic input power to electrical power generated is 89% for a much occurring sea states of $T_e=10,5s$; $H_s=2.25m$. This includes the full Symphony operation in irregular waves, bi-directional flow, PTO rotational speeds from 0 tot 350 rpm.

The next step is to verify the calculated efficiency curve with experimental data. A test program is setup using the physical prototype of the PTO (see Deliverable D4.2). First results are expected in June 2018. Running the PTO manually and dry shows a very smooth and frictionless rotation, but tests with water under pressure have to show the final verification of the calculations.

1. Introduction to Symphony

1.1 Operating Principle

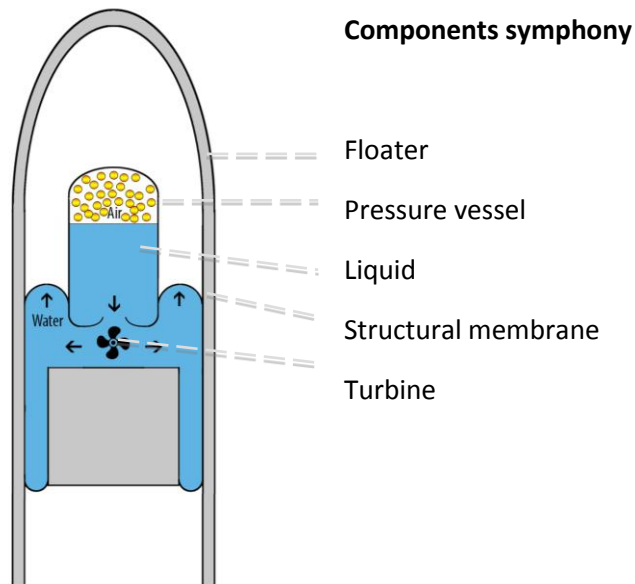


FIGURE 1: DIFFERENT PARTS OF THE SYMPHONY

floaters. This force counteracts the force, caused by pressure field in the wave. By counteracting this force during the motion, energy is drawn from the waves through mechanical energy into electricity in the generator.

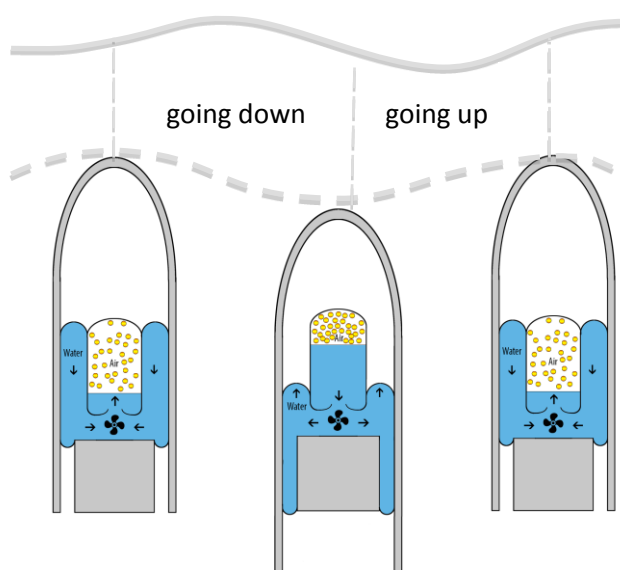


FIGURE 2: OPERATING PRINCIPLE OF THE SYMPHONY

In a high pressure field, under a wave, the upper side (floater) of the symphony goes down. In a lower pressure field, wave trough, the pressure, in the internal pressure vessel pushes it up again. The liquid inside acts as a medium and is displaced and pushed in and out the pressure vessel and into the structural membrane. This liquid stream is pushed through a special purpose turbine. The blades in the turbine start to rotate as the liquid goes through. The turbine makes a generator rotate (not in the picture). The current in the generator creates a magnetic force and builds a torque that, in the turbine builds up a pressure over the blades of the turbine. This pressure counteracts the motion and through the structural membrane, the force acting on the

The pressure in the pressure vessel is build up as the volume of gas decreases. There is a direct relation between the position of the floater and the pressure in the pressure vessel. The resulting force as function of this internal pressure acts as a spring force

The mass of the floater and the moving water and the inertia of the turbine and generator, have to accelerate and decelerate during this motion.

Consequently, the whole system acts as a damped mass spring system. If the natural frequency of the system is equal to the wave frequency, the system will resonate

with the wave pressure and the motion of the floater is attenuated. The generator through the turbine has to take energy from this attenuated motion to keep it between its mechanical end buffers.

A study on different control schemes and optimal energy absorption for the Symphony was done [1]. It shows that for optimal energy abstraction the motion of the Symphony should be in a constant phase shift with the wave. Under the wave top the floater should be at its highest velocity, going down. Under a wave trough the floater should move up.

The device swings up and down. During this motion kinetic energy (moving mass) is constantly transferred into potential energy (spring) for a constant stroke the energy is constant. So at every position potential energy added with kinetic energy is a constant number. As the velocity and position are constant measured the change of energy in the system is known at any moment. If the energy in the system increases (higher velocities) this means the system is capturing energy from the waves. This energy is tapped from the moving system by the generator, by applying a torque on the turbine wheel and slowing down the velocity of the liquid.

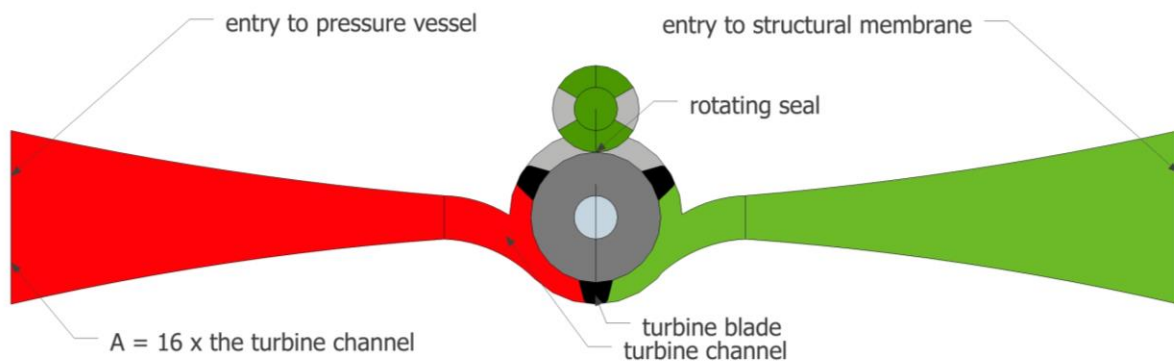


FIGURE 3: TURBINE VENTURI STRETCHED

For the turbine characteristics, this gives a non typical characteristic. Since normally a turbine is build to take as much energy out of the liquid, by building pressure and slowing down the liquid. In the case of symphony the first criteria is to allow liquid to flow from the membrane into the pressure vessel and visa versa to secure a spring function. For this, much attention went to the venturi or the tapered channel from the pressure vessel to the turbine. A 4 degree angle was taken so that the area at entry is 16 times larger than near the blades. Towards the structural membrane the same slope is taken. So the

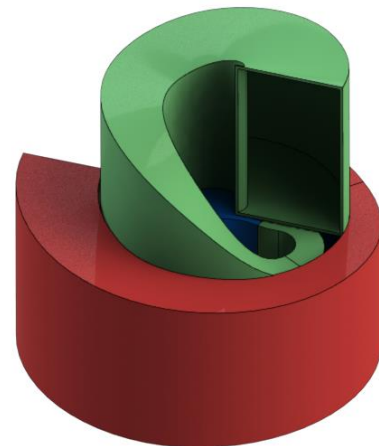


FIGURE 4: TURBINE VENTURI

highest velocities of ca 7m/s are slowed down to 0.4 m/s before exit as can be seen in figure 3. The pressure drop at entry is therefore limited. As there was no space for this tapered channel in the linear space, the shape is curved as seen in figure 4.

Not only the channel should be well profiled, also the turbine should have very little friction. For this, the design uses only one seal. All bearings in the turbine are water lubricated ceramic bearings. Also the gearbox synchronizing the rotating seal with the rotor run in water. In figure 5, the interior of the rotor is given.

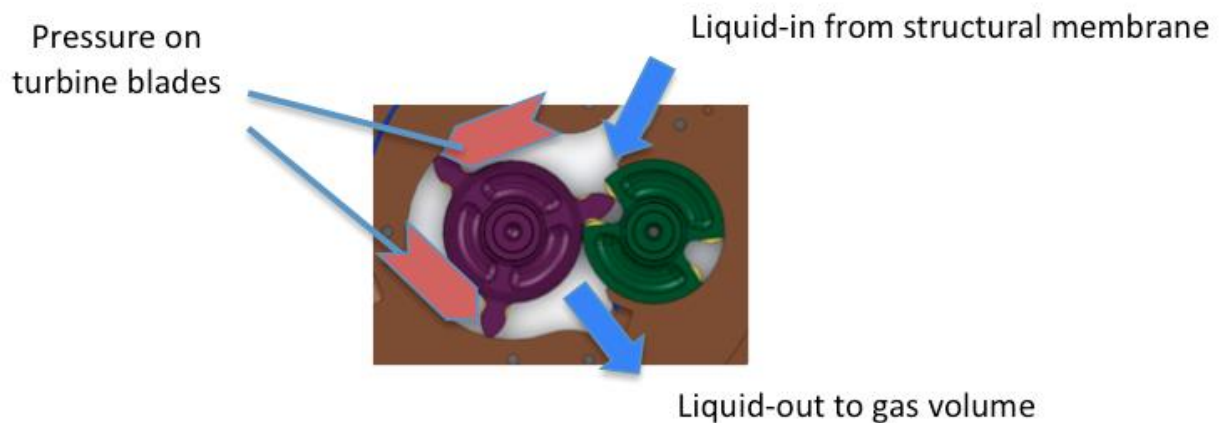
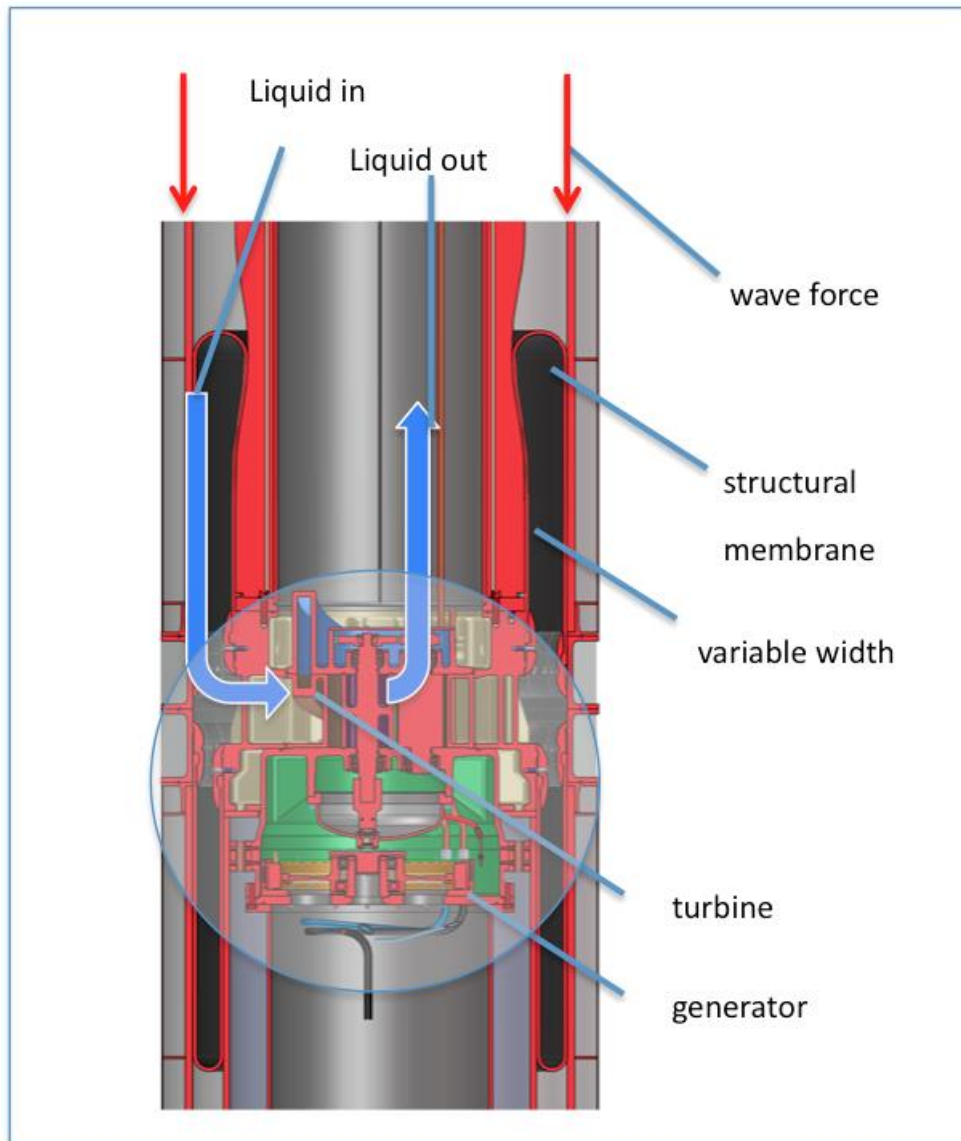


FIGURE 5: TURBINE CROSS SECTION

The rotor should run as smooth as possible. Only if the velocity of the floater is above the typical velocity defined in the control for each position, the turbine has to build up pressure and slow down the floater. As the higher velocity of the floater is in direct relation with the wave height, the installed pressure over the turbine has a direct relation with the wave height. This wave height is however not measured in situ for control purpose. The behavior of the device has a direct relation to the wave acting and is the main indicator to the control of the pressure over the turbine. Of course the waves are measured near the device to characterize the sea state and to evaluate the power conversion efficiency. Figure 6 shows the operating principle of the PTO of the Symphony.



FIGUUR 6: OPERATING PRINCIPLE PTO

1.2 The Generator

The generator has a direct connection to the rotor as seen in figure 7. So there is no gearbox. This, however, means that the generator has to speed up and speed down within a few seconds. This adds to the inertia of the system. The energy for accelerating and deceleration does not come from the electrical current; the energy is imposed by the gas-spring in the pressure chamber and is induced on the turbine blade as an extra torque. The generator is a permanent magnet generator with magnets on the rotating part. The stator is cooled by water. For this, at both sides of the turbine a small connection is made, at which two tubes lead the water to the cooling body of the stator. A small flow runs parallel of the turbine through the generator. By doing so no extra pumps are needed.

The voltage from the generator is induced by the magnets and is high at high velocity. The output with a constantly changing voltage is connected to an IGBT converter. This unit controls the current by high frequency IGBT switches. This current is fed into a DC voltage link. From this DC voltage the current (energy) is going into the next level. In case of an AC grid, a second IGBT converter takes care of the discharge from the DC voltage link into the grid. Other options are, to use the DC link to interconnect several systems.

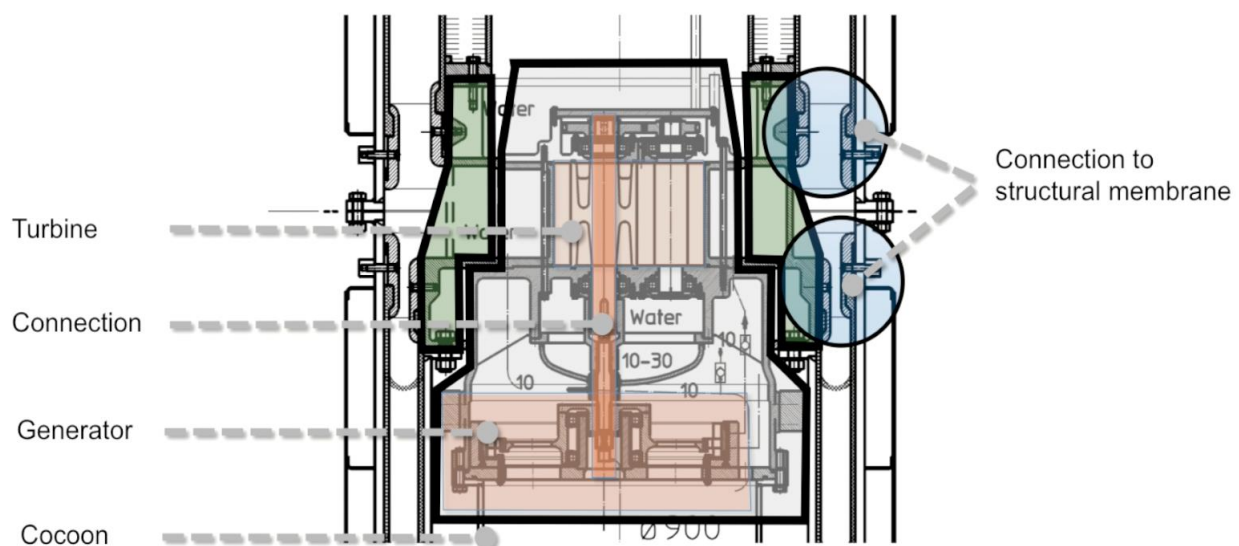


FIGURE 7: THE PTO OF THE SYMPHONY

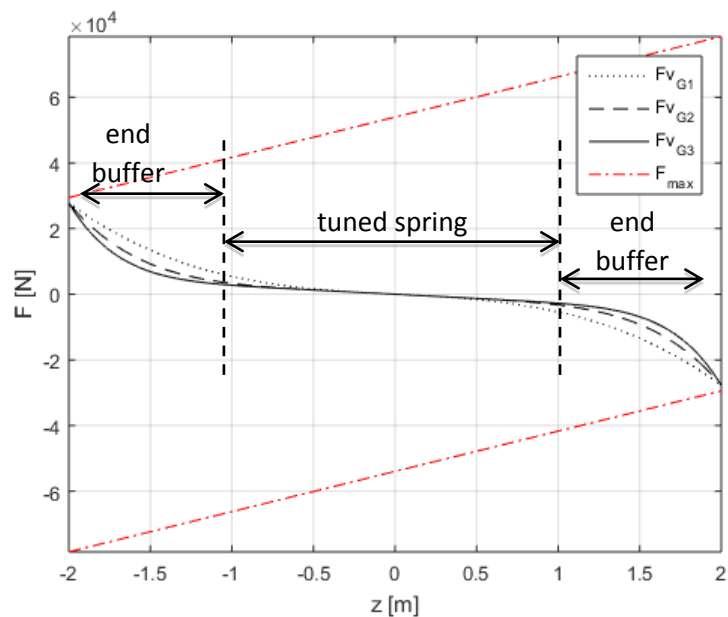
The PTO of the Symphony uses a permanent magnet synchronous alternator (PMSG) with a rated power of 22kW as generator. To find more cost-efficient options for future designs a research was conducted [2]. There is some research available on generator designs for wave energy converters but the Symphony is a unique case, so a new research needed to be done. Several generator types can be used in the Symphony. Compared to an induction and switched reluctance generator, the iron-cored permanent magnet synchronous generator (PMSG) seems a good choice because it is efficient and reliable. A disadvantage, however, is that, in the case of the Symphony, the iron losses are relatively high at partial loads. An air-

cored PMSG does not have this problem since it has no iron losses at all. A drawback of the air-cored PMSG is that it needs more permanent magnetic material, which is expensive. Finally, it was decided to test and compare the iron-cored radial flux PMSG and the air-cored axial flux PMSG on both performance and costs. For both generator types, an analytical model was built which puts out the efficiency and material cost. To find the best generator geometries for the case of the Symphony, an optimization procedure was created which minimizes both material costs and losses. It was found that an axial flux air-cored PMSG is both cheaper and more efficient than a radial flux iron-cored PMSG. The iron losses of an iron-cored generator are relatively high at partial loads while the Symphony operates at partial loads most of the time.

1.3 The end buffers

The system behaves as an attenuated mass spring system. This means that each time a wave passes, the oscillating motion is attenuated more. A continuous small wave can cause a motion that is several times more than the wave height. If the motion is not damped (slowed down by taking energy out through the generator) the motion will increase and start hitting its mechanical end stops. Normally the generator takes the energy from the motion and keeps it from hitting the end buffers. In the highest sea states (H_s 4.5 with waves up 9 m) the wave energy exceeds the capability of the generator. Increasing the size of the generator and the turbine for incidental waves of this size is not economical viable. It is better to have another mechanism to reduce the system from making larger motions. In Symphony the shaping of the channel (gap) in which the structural membrane rolls creates a large force slowing down the motion. This force is position dependent and can therefore be seen as a spring or a buffer. If the floater runs into this buffer, it does not dissipate the energy. Instead, it charges the spring and pushes the floater back. This fast response brings the floater out of synchronicity with the waves, the force is low and no heat is dissipated. This intrinsic protection is designed so that with the highest waves and loss of grid the system is not in danger. As such, it creates an intrinsic protection. A study has been conducted in order to determine the optimal shape of the channel for the membranes [3].

The graph above shows the spring characteristic as a force as function of the position of the floater.



In this function, not only the shape of the gap, but also the internal pressure in the pressure vessel and the water column on top of the floater are taken into account.

The structural membrane works as a bearing as well. Because the central pushing force is a function of the surface, over which the membrane touches the middle cylinder, a more narrow gap on one side will create a force to widen up the gap again, and a such a very stiff spring centralizing both bodies. In the axial direction the motion is very smooth, apart from the spring force programmed in the shape. (see spring function) Apart from sealing the interior from the outside seawater the structural membrane acts as a efficient bearing as well.

1.4 Time-Domain Model

To create the functions described above the numbers should fit. These numbers are calculated in several models and brought together in a time domain model. With this model the motion, forces and power levels can be simulated. In figure 8 a block diagram of this model is given.

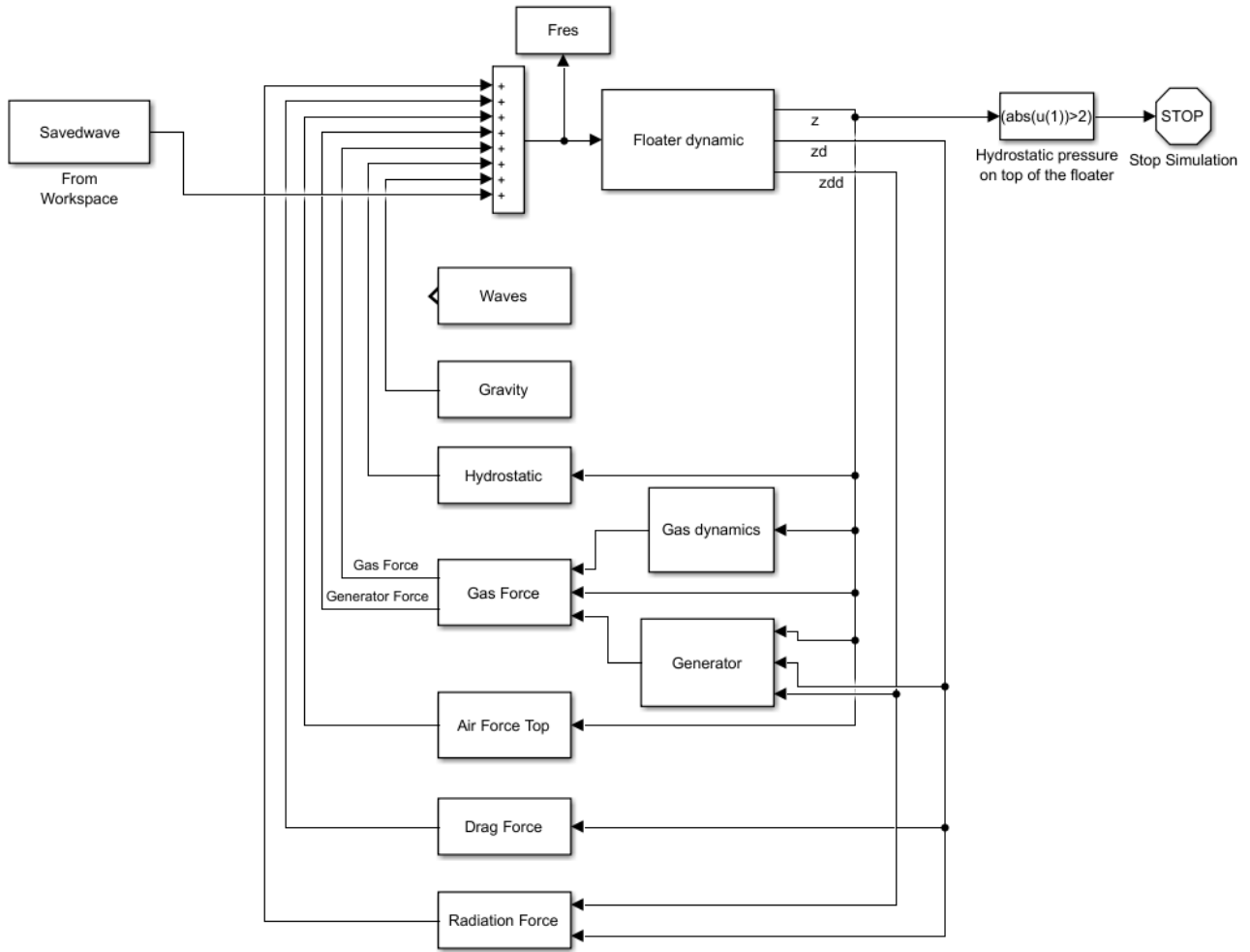


FIGURE 8: SCHEMATIC REPRESENTATION OF THE TIME-DOMAIN MODEL

In the diagram below all forces moving the mass are identified. Here also the two turbine forces are identified. Not only the absolute forces, but also the forces in time. As an input statistical data is taken from the scatter diagram of a certain location.

In the time-domain model, the position (z), the speed (z_d) and the acceleration (z_{dd}) of the floater of the Symphony are calculated. This is done by summing up all the forces that are present in the Symphony according to equation 1.

$$m\ddot{z} = F_{Wave}(t) + F_G + F_{HS}(z) + F_{Gas}(z) + F_{AirTop}(z) + F_{PTO}(\dot{z}, z) + F_D(\dot{z}) + F_{Rad}(\dot{z}) \quad (1)$$

Where:

- m is the mass of the floater [kg]
- z is the position of the floater [m]
- \dot{z} is the velocity of the floater [m/s]
- \ddot{z} is the acceleration of the floater [m/s²]
- F_{Wave} is the wave force on top of the floater [N]

- F_G is the gravitational force on the Symphony [N]
- F_{HS} is the hydrostatic force on top of the floater [N]
- F_{Gas} is the gas force due to compression in the spring chamber [N]
- F_{AirTop} is the spring force below the floater [N]
- F_{PTO} is the breaking force of the PTO [N]
- F_D is the drag force due to the movement through the water [N]
- F_{RAD} is the radiation force due to moving the floater in inviscid fluid [N]

2. Description of the PTO

The turbine developed for the Symphony is based on a positive displacement pump. It consists of two runners with a crosssection as shown in figure 9. The rotors are coupled by a set of gear wheels. The axis of the larger rotor extends out of the casing and is coupled to the generator. A study has been done to determine the optimal dimensions of this turbine [4].

The water flowing to and from the symphony membrane system, that is led into the turbine, makes the rotor turn thus driving the generator. The second rotor serves to block the flow at the other side of the larger rotor. It is driven at 50 % higher speed and in the opposite direction from the larger one.

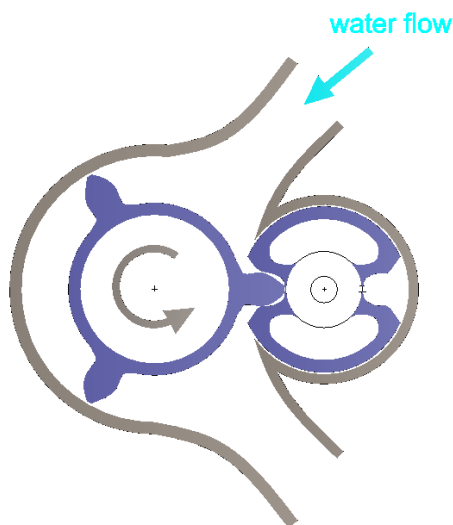


FIGURE 9: CROSS SECTION OF THE TURBINE

Inlet and outlet are connected to special shaped diffusors to reduce entrance and exit losses as seen in figure 10.

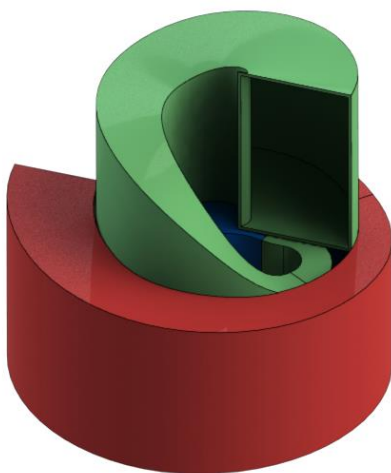


FIGURE 10: IN AND OUTLET DIFFUSORS

Here the flow in one direction is given. In operation however the flow reverses continuously. As the turbine is in a high degree symmetrical the results for one direction are also applicable for the other one.

2.1 Theoretical Efficiency

The following section shows the theoretical determined efficiency of the turbine. The property discussed here is the efficiency under different loads and speeds of the turbine.

The gross power produced by the turbine is given by equation 2:

$$P_g = \Delta p \cdot \phi \quad (2)$$

Where:

- P_g is the gross power extracted from the flow [kW]
- Δp is the inlet pressure minus the outlet pressure [Pa]
- ϕ is the liquid flow [m³/s]

The gross torque follows from equation 3:

$$T_g = \frac{P_g}{(2 \cdot \pi \cdot \frac{n}{60})} \quad (3)$$

Where:

- T_g is the gross torque on the shaft [Nm]
- n is the rotational speed of the turbine [rpm]

Efficiency losses occur as a result of leakage flows in the turbine as a result of the gaps between the runners and the housing. There are different types of losses during the passage of the flow through the turbine which is represented in figure 11.

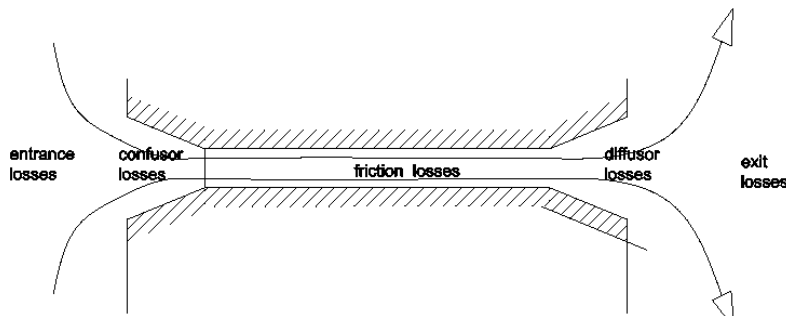


FIGURE 11: LOSSES WITHIN THE GAPS

The effect of a number of different hydraulic losses on the efficiency of the turbine are considered :

- Entrance loss (head loss)
- Loss in the inlet confuser (head loss)
- Loss due to slip of flow along the runners (speed loss)
- Loss due to flow friction (turbulent or laminar) around the runners (torque loss)

- Loss in the outlet diffuser (head loss)
- Exit loss (head loss)

All losses can be seen as loss of exit power to compute the overall efficiency. The head losses are multiplied by the water flow, the speed loss by the gross torque and the torque loss by the gross speed (radians/s).

2.1.1 Slip losses

First the slip losses are considered. Slip occurs at different locations. In figure 10 the different leak ways within the turbine are shown.

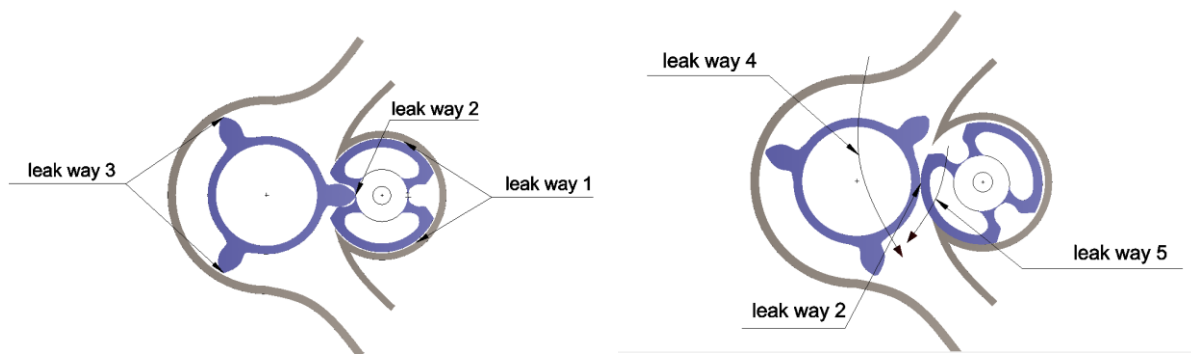


FIGURE 12: DIFFERENT LEAK WAYS WITHIN THE TURBINE

Leak way 1 is the narrow gap around the smaller runner. Leak way 2 is between the two runners, either across the top to the tooth of the larger runner or between the cylinder shapes of the two runners. Leak way 3 is across the teeth of the larger runner and the housing. Further more there are leak ways over and under the end surfaces of the runners (4 and 5).

The flow through these leak ways have a different character. The flow through the long narrow gap of leak way 1 is a laminar poiseuille flow. In that case the entrance and exit losses are negligible compared to the viscous resistance in the gap. The flow through the other leak ways are short gaps, which means that there the entrance and exit losses dominant.

Leak way 1

The laminar flow through leak way 1 is complex as one of the walls (runner) moves, while there is also a pressure drop along the gap. This is shown in figure 13.

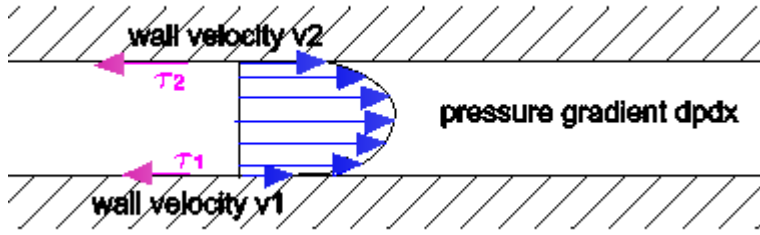


FIGURE 13: VELOCITY PROFILE OF LEAK WAY 1

Analys shows that the wall stress is :

$$\tau_1 = \eta \cdot \frac{(v_2 - v_1)}{s} + \frac{dpdx \cdot s}{2} \quad (4)$$

Where:

- τ_1 is the shear stress on the wall [N/m²]
- v_1 is the velocity of wall 1 [m/s]
- v_2 is the velocity of wall 2 [m/s]
- s is the width of the gap [m]
- $dpdx$ is the pressure gradient [Pa/m]

In this case where $v_2=0$ this equation simplifies to:

$$\tau_1 = \eta \cdot \frac{v_1}{s} + \frac{dpdx \cdot s}{2} \quad (5)$$

This can be either negative or positive depending on the relative magnitude of the rotational speed and the pressure drop.

The mean velocity in the gap is :

$$v_{mean} = \frac{(v_1 + v_2)}{2} - \frac{1}{12} \cdot \frac{dpdx}{\eta} \cdot s^3 \quad (6)$$

Hence the flow through the gap is :

$$\Phi_1 = v_{mean} \cdot s \cdot h$$

Where:

- h is the height of the rotor [m]

For such a long and narrow gap, these friction losses are dominant and the other losses can be neglected.

The resulting power loss is:

$$Slip\ loss_1 = dp_{turbine} \cdot \left(\frac{(v_1 + v_2)}{2} + \frac{1}{12} \cdot \frac{dp_{dx}}{\eta} \cdot s^3 \right) \cdot s \cdot h \quad (7)$$

This is not the case for the other leak ways. As the channels are very short there, the entrance and exit losses are dominant and friction can be neglected.

Both entrance and exit losses are computed as :

$$dp_{loss} = \xi \cdot \frac{1}{2} \cdot \rho \cdot v^2 \quad (8)$$

or :

$$v = \sqrt{\frac{2 \cdot dp_{loss}}{\xi \cdot \rho}} \quad (9)$$

Where:

- v is the velocity of the fluid [m/s]
- dp_{loss} is the pressure loss [Pa]
- ξ is the discharge coefficient [-]
- ρ is the density of the medium [kg/m³]

For all leak ways the same values for ξ have been chosen: 0.5 for the entrance losses and 1.0 for the exit losses.

Leak way 2

This case is the more complex one. Most part of the time the flow is blocked by the gap between the two cylindrical runners and now and then by the gap between the tip of the “tooth”.

For both cases the same gap width has been assumed.

$$Slip\ loss_2 = dp_{turbine} \cdot \sqrt{\frac{2 \cdot dp_{turbine}}{1.5 \cdot \rho}} \cdot s \cdot h \quad (10)$$

Leak way 3

This is the leak way at the other side of the larger runner. As can be seen from figure 10, most of the time the flow is blocked here by two teeth in series, each with the same pressure drop across it.

Hence the loss is :

$$Slip\ loss_3 = dp_{turbine} \cdot \sqrt{\frac{2 \cdot \frac{dp_{turbine}}{2}}{1.5 \cdot \rho}} \cdot s \cdot h \quad (11)$$

Leak way 4

The geometry of the runners at the top and bottom are shown in figure 14.

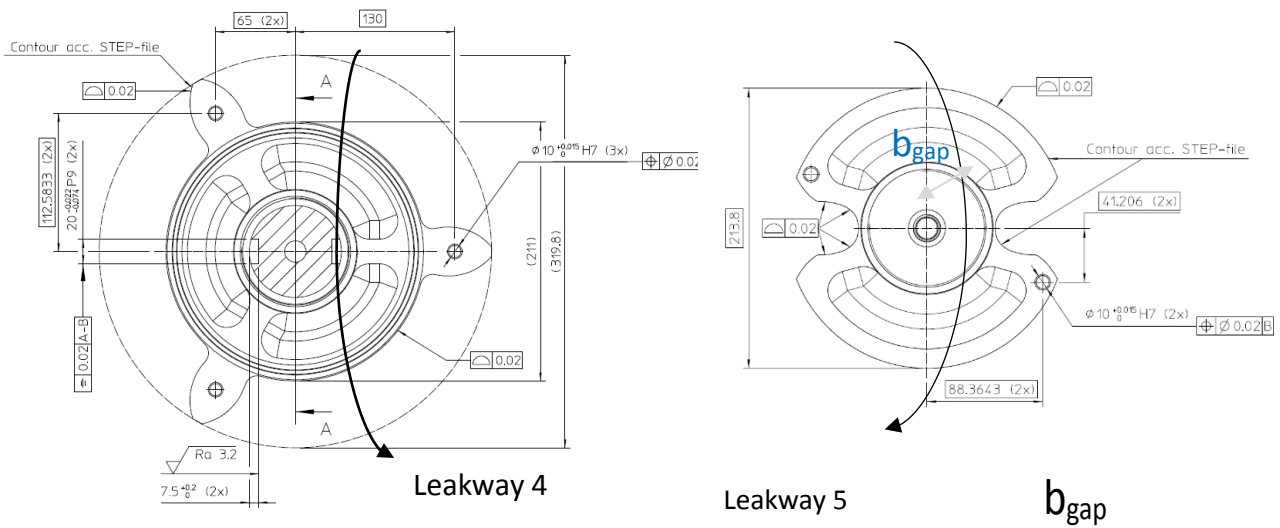


FIGURE 14: TOP VIEW RUNNERS

The flow under and over the runner passes two restrictions (the wall of the runner) . The breadth of these gaps is a third of the circumference of this wall.

The loss in leak way 4 (top and bottom) is thus:

$$Slip\ loss_4 = 2 \cdot dp_{turbine} \cdot \sqrt{\frac{2 \cdot \frac{dp_{turbine}}{2}}{1.5 \cdot \rho}} \cdot s \cdot \frac{2\pi}{3} \cdot d_{runner} \quad (12)$$

Where:

- d_{runner} is the diameter of the runner [m]

Leak way 5

The leak way across the smaller runner runs from the outside into the runner. Has then to pass into the small channel that encloses the tooth and out again.

These latter passages form the main resistance of this leak way. The assumed width is given in figure 12.

Leak flow 5 is therefore:

$$Slip\ loss_5 = 2 \cdot dp_{turbine} \cdot \sqrt{\frac{2 \cdot \frac{dp_{turbine}}{2}}{1.5 \cdot \rho}} \cdot s \cdot b_{gap} \quad (13)$$

Where:

- b_{gap} is the width of the gap [m]

2.2.2 Friction Loss

In addition to the slip losses there are also friction losses: mechanical friction in seals and bearings (not considered here) and the laminar friction loss in leak way 1.

As mentioned above the combination of rotation and pressure drop exerts a shear stress on the cylindrical surface resulting in a torque on that runner.

This torque is :

$$\Delta T = \left(\eta \cdot \frac{v_1}{s} - \frac{dp_{dx} \cdot s}{2} \right) \cdot \frac{2}{3} \pi \cdot D_l \cdot \frac{D_l}{2} \quad (14)$$

The power dissipated (or generated) is given by:

$$\text{Torque power loss} = - \Delta T \cdot \omega = - \Delta T \cdot 2 \pi \frac{rpm}{60} \quad (15)$$

2.1.3 Confusor and Diffusor Losses

For a given flow direction, the entrance diffusor acts as a confusor, accelerating the flow instead of decelerating it. The one at the exit really acts as a diffusor, slowing down the flow to reduce the exit losses.

The losses in an accelerating flow are much lower than in a decelerating flow. Therefore, the losses in the confusor are neglected in this analysis.

The entrance losses of the confusor and the exit losses of the diffusor are so low that they too can be neglected, leaving the loss of the diffusor.

This loss is also expressed in the general form :

$$dp_{loss} = \xi \cdot \frac{1}{2} \cdot \rho \cdot v^2 \quad (16)$$

Where :

v = the velocity at the entrance of the diffuser. For the chosen geometry the value of $\xi = 0.04$.

2.1.4 Overall Evaluation

The efficiency is computed as:

$$\eta = \frac{P_{gross} - \sum P_{losses}}{P_{gross}} \quad (17)$$

The efficiency depends on the value of the gross power generated and the speed of the turbine.

This relation was evaluated in a Matlab script for the Symphony geometry and resulted in the graph given in figure 15.

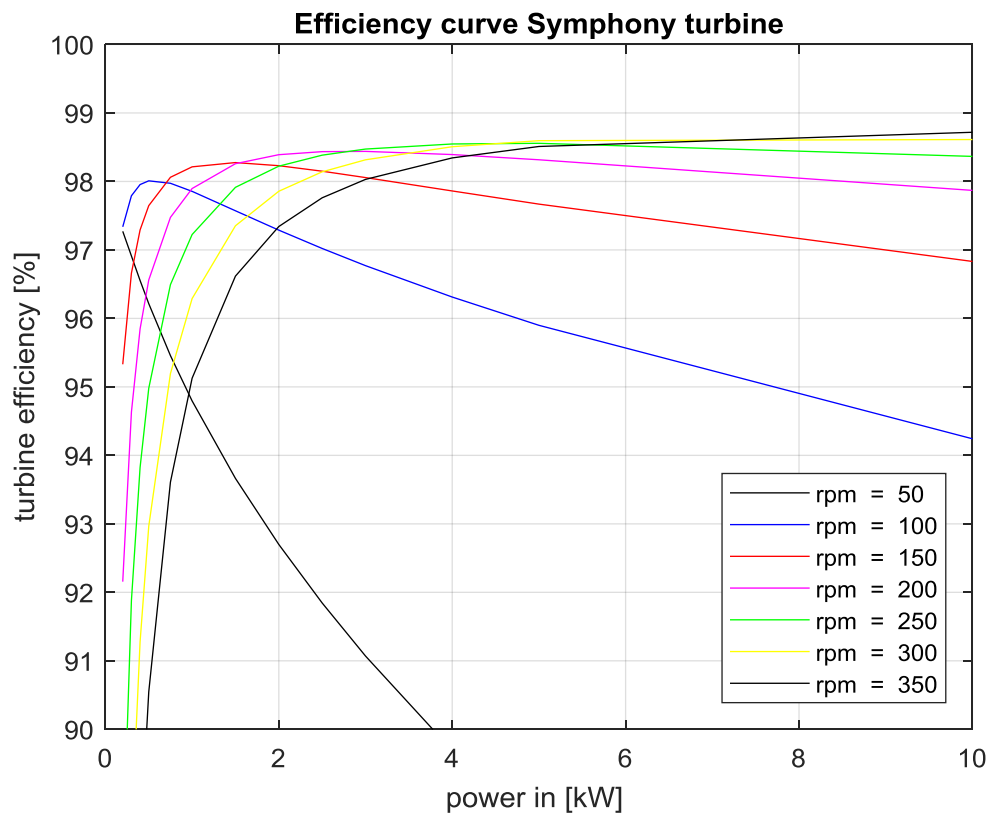


FIGURE 15: THEORETICAL EFFICIENCY OF THE TURBINE

Dimensions relevant for assessing the efficiency are:

- Water content per revolution of the larger runner = 0.13 m³
- Nominal speed = 350 rpm
- Nominal pressure drop = 3 bar
- Dimensions of the runners
- Dimensions of the diffusers

From equations (2) and (3) follows:

$$P_g = 3 \cdot 10^5 \cdot 0.13 = 39 \text{ kW}$$

$$T_g = \frac{39 \text{ kW}}{(2 \cdot \pi \cdot \frac{350}{60})} = 1064 \text{ Nm}$$

2.2 PTO conversion efficiency in realistic sea state conditions

The turbine characteristics have been implemented in the time domain model (see chapter 1.4) of Symphony. In the matrices below (figures 16 and 17), the power at three steps in the wave to wire conversion of the PTO is given.

First (figure top figure of figure 16) the average power captured by the system is for each T_e/H_s combination is given as mechanical power. This is the net power that moves the outer structure up and down. The radiated wave and drag of the system through the water is subtracted. The hydraulic power from the waves is not taken into account since the $\frac{1}{4}$ scale device (1,5m dia) is very small compared to the wave. Comparing with the wave power per meter wave does not give relevant information in this respect.

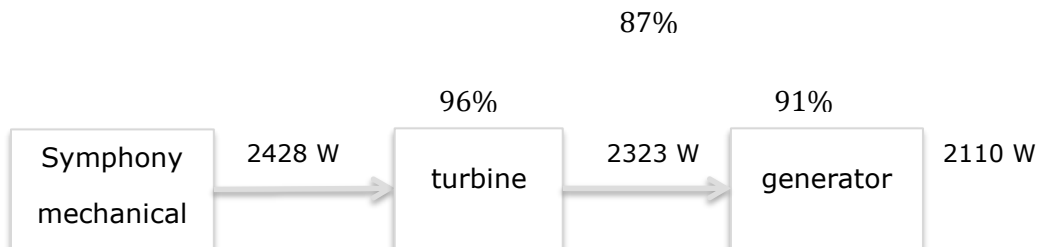
In the second step (middle matrix in figure 16) gives for each T_e/H_s combination the power converted by the Turbine and applied at the generator.

In the third step (bottom picture in figure 16) the time domain model calculates the power delivered the grid for each sea state.

So for each sea state (T_e/H_s combination), two conversion steps are calculated. By using the time domain model, all waves in the sea state are taken into account. But also the 2-directional flow, the full stroke and related rotational speeds etc.

The block diagram below shows an example for one sea state and explains how figure 16 and 17 must be read. The example below is for a sea state much occurring and representative for the sea state Symphony and many other WEC's are aiming at.

So we take the sea state $H_s = 2,25 \text{ m}$ and $T_e = 10,5 \text{ s}$, for the two steps described above, the conversion is given below. Step one is with a conversion of 96% and step two with 91%. The total conversion is the product, 87%.



The total internal conversion efficiency of the system is **87%** in this representative sea state.

The tables in figure 16 and 17 give the PTO conversion efficiency for all sea states between $T_e=4,5s$; $H_s=0,75m$ and $T_e=14,5s$; $H_s=4,25m$. Depending on the location and its scatter diagram the conversion as function of the location can be estimated.

Average Hydraulic power into the Turbine (W)								
Te\Hs	0,75	1,25	1,75	2,25	2,75	3,25	3,75	4,25
4,5	920,2	2175,5						
5,5	869,9	1563,1	2094,5	2833,4				
6,5	838,6	1547,3	2063,8	2645,8	3529,6	4314,4		
7,5	863,6	1343,5	1931,7	2477,0	3006,0	4282,5	5537,3	5946,4
8,5	763,2	1358,2	1790,2	2677,9	3119,8	4300,7	4823,7	6619,8
9,5		1059,0	1773,0	2500,7	3558,3	3686,6	5006,6	4808,3
10,5		1101,1	1883,8	2428,1	3085,3	3072,4	4256,2	6624,5
11,5		1014,3	1553,8	2255,2	3082,4	3480,6	3854,5	3768,3
12,5				2397,3	2745,3	3457,9	4546,9	4736,0
13,5					2529,5	2617,3	3984,5	6211,8
14,5								3473,1
15,5								
16,5								

Average mechanisch power turbine out and genrator in (W)								
Te\Hs	0,75	1,25	1,75	2,25	2,75	3,25	3,75	4,25
4,5	550,8	1432,0						
5,5	553,4	1156,7	1633,7	2393,9				
6,5	604,3	1255,4	1820,3	2365,0	3243,1	4028,8		
7,5	677,3	1146,5	1727,5	2276,0	2800,4	4070,0	5431,6	5734,8
8,5	647,1	1230,4	1638,4	2529,6	2953,1	4134,1	4667,8	6450,8
9,5		948,6	1673,9	2383,6	3434,1	3547,4	4870,5	4684,6
10,5		1029,2	1796,0	2322,9	2971,3	2960,6	4119,5	6503,9
11,5		948,7	1489,1	2163,8	2986,2	3363,6	3758,4	3684,7
12,5				2315,6	2647,8	3353,2	4409,5	4616,2
13,5					2437,1	2523,1	3865,3	6091,1
14,5								3363,8
15,5								
16,5								

Average electrical power, generator out (W)								
Te\Hs	0,75	1,25	1,75	2,25	2,75	3,25	3,75	4,25
4,5	459,7	1257,2						
5,5	452,0	1005,6	1447,3	2155,1				
6,5	500,6	1096,7	1624,9	2140,1	2971,4	3714,5		
7,5	557,9	999,0	1547,8	2054,8	2560,2	3757,0	5045,1	5328,8
8,5	530,0	1077,5	1467,9	2303,9	2700,2	3821,3	4320,9	6005,5
9,5		816,0	1500,3	2168,0	3155,8	3266,9	4512,9	4344,2
10,5		898,5	1615,8	2110,0	2726,6	2712,5	3801,1	6060,1
11,5		822,3	1331,4	1968,5	2733,4	3093,2	3467,9	3416,7
12,5				2106,6	2419,0	3085,6	4073,7	4270,2
13,5					2221,4	2304,5	3561,4	5663,5
14,5								3094,6
15,5								
16,5								

FIGURE 16: FOR A SERIES OF SEA STATES IN THREE STEPS THE ENERGY INPUT IS GIVEN FROM WAVE TO ELECTRICAL POWER. THE CONVERSION FROM STEP 1 TO 2 AND FROM 2 TO 3 IS GIVEN IN FIGURE 17.

Average turbine efficiency								
Te\Hs	0,75	1,25	1,75	2,25	2,75	3,25	3,75	4,25
4,5	60%	66%						
5,5	64%	74%	78%	84%				
6,5	72%	81%	88%	89%	92%	93%		
7,5	78%	85%	89%	92%	93%	95%	98%	96%
8,5	85%	91%	92%	94%	95%	96%	97%	97%
9,5		90%	94%	95%	97%	96%	97%	97%
10,5		93%	95%	96%	96%	96%	97%	98%
11,5		94%	96%	96%	97%	97%	98%	98%
12,5				97%	96%	97%	97%	97%
13,5					96%	96%	97%	98%
14,5								97%
15,5								
16,5								

generator efficiency								
Te\Hs	0,75	1,25	1,75	2,25	2,75	3,25	3,75	4,25
4,5	83%	88%						
5,5	82%	87%	89%	90%				
6,5	83%	87%	89%	90%	92%	92%		
7,5	82%	87%	90%	90%	91%	92%	93%	93%
8,5	82%	88%	90%	91%	91%	92%	93%	93%
9,5		86%	90%	91%	92%	92%	93%	93%
10,5		87%	90%	91%	92%	92%	92%	93%
11,5		87%	89%	91%	92%	92%	92%	93%
12,5				91%	91%	92%	92%	93%
13,5					91%	91%	92%	93%
14,5								92%
15,5								
16,5								

Total internal system efficiency								
Te\Hs	0,75	1,25	1,75	2,25	2,75	3,25	3,75	4,25
4,5	50%	58%						
5,5	52%	64%	69%	76%				
6,5	60%	71%	79%	81%	84%	86%		
7,5	65%	74%	80%	83%	85%	88%	91%	90%
8,5	69%	79%	82%	86%	87%	89%	90%	91%
9,5		77%	85%	87%	89%	89%	90%	90%
10,5		82%	86%	87%	88%	88%	89%	91%
11,5		81%	86%	87%	89%	89%	90%	91%
12,5				88%	88%	89%	90%	90%
13,5					88%	88%	89%	91%
14,5								89%
15,5								
16,5								

FIGURE 17 : TOP TWO DIAGRAMS SHOW THE CONVERSION BETWEEN STEP 1 → 2 AND FROM STEP 2 → 3 OF FIGURE 16. THE THIRD DIAGRAM SHOWS THE OVERALL CONVERSION PER SEA STATE FROM WAVE INPUT TO ELECTRICAL OUTPUT.

2.3 Turbine Testing

In order to measure the efficiency of the turbine, a test setup is being built. The goal of this setup is to measure the efficiency as a function of pressure difference and rotational speed.

2.3.1 Theoretical Loss Components

The losses described in the previous chapter can be divided into hydraulic losses and mechanical losses.

The hydraulic losses are a result of losses in flow. Assuming a laminar leakage flow, these losses can be described according to the following equations:

$$Q_1 - \frac{p_1}{C_{e1}} - \frac{p_1 - p_2}{C_i} - D\omega = 0 \quad (18)$$

$$D\omega - \frac{p_1 - p_2}{C_i} - \frac{p_2}{C_{e2}} - Q_2 = 0 \quad (19)$$

Where:

- Q_1 is the input flow [m^3/s]
- Q_2 is the output flow [m^3/sp]
- p_1 is the pressure at the input [Pa]
- p_2 the pressure at the output [Pa]
- ω is the rotational speed [rad/s]
- D is the theoretical volumetric displacement [m^3/rad]

The leakage flow from the input to the output is characterised by leakage coefficient C_i . The leakage flow to the exterior from the input and output are characterised by leakage coefficients C_{e1} and C_{e2} respectively.

The mechanical losses are a result of loss of torque on the shaft. The losses can be described using the following equation:

$$T_L = D(p_1 - p_2) - B\omega - \frac{\omega}{|\omega|} C_f D(p_1 - p_2) - \frac{\omega}{|\omega|} T_{c0} \quad (20)$$

Where:

- T_L is the torque at the generator shaft [Nm]

The viscous damping losses are characterised by damping coefficient B . The internal friction of the turbine is characterised by the internal friction coefficient C_f . Finally, there is a constant torque loss, T_{c0} , which is the torque to overcome the friction in the seals.

In summary, six loss components were identified which should be found during the turbine tests. These loss components are shown in table 1.

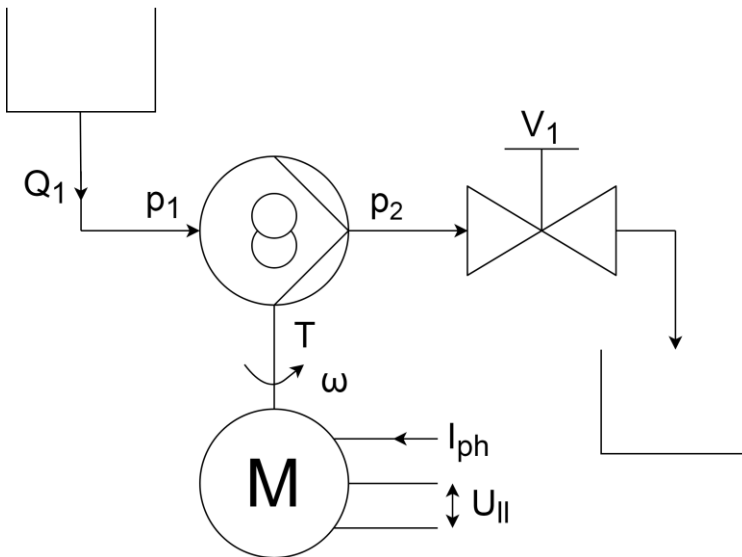
TABLE 1: DIFFERENT LOSS COMPONENTS

Loss Component	Coefficient	Proportional to
Internal leakage loss	C_i	Pressure difference
External input leakage loss	C_{e1}	Input pressure
External output leakage loss	C_{e2}	Output pressure
Viscous damping loss	B	Rotational speed
Internal friction loss	C_f	Pressure difference
Constant torque loss	T_{c0}	N/A

Since the loss components are independent of the direction of power flow, the loss coefficients of the turbine can also be determined when the turbine is tested as a pump. For convenience it has been chosen to test the turbine as a pump and to drive it with the generator as a motor. In this configuration, no external pump is needed to generate a pressure difference.

2.3.2 Test Setup and Instrumentation

The turbine will be tested in the water laboratory in the faculty of Civil Engineering and Geosciences at the Delft University of Technology. In the laboratory there is a connection to a water basin available as well as an electrical connection to the grid. A schematic overview of the test setup is shown in figure 18.


FIGURE 18: SCHEMATIC REPRESENTATION OF THE TEST SETUP

The input of the turbine is connected to the water basin. The flow through the turbine will be measured with a flow meter. The flow meter is placed at the input of the turbine. The pressure difference over the turbine is measured by two separate pressure sensors. . These sensors are placed at the input and output of the turbine. Also the pressure at the beginning and end of the diffusers is measured, so the efficiency of the diffusers is determined separately.

The shaft of the turbine is directly connected to the shaft of the generator. By adjusting the rotational speed, the amount of flow can be set. The rotational speed of the turbine is measured by an incremental encoder. Incremental encoders give a certain amount of pulses per revolution. The accuracy of this kind of encoders is close to 100%. The torque cannot be measured directly. The torque will be calculated by measuring the power provided to the motor. This is done by measuring the phase current and line-to-line voltage. The losses in the motor have been characterised separately. Finding the torque with the method above is robust, but depends on the currency of a number of measurements. This system accuracy should be taken into account

At the output of the turbine, a valve is installed. By adjusting the valve, a pressure difference over the turbine can be set.

2.3.4 Test Plan

Since the main goal of these measurements is to find the efficiency as a function of pressure and rotational speed, finally, a graph will be made which plots these parameters. The different loss components will be found according to the following steps:

- The first loss component to be determined is the constant torque loss. With a torque wrench on the shaft, the amount of torque loss can be measured. The amount of constant torque loss is expected to be negligible, however.
- Secondly, the hydraulic losses will be measured. With valve V_1 closed and the turbine rotating very slowly, the amount of leakage flow is determined by comparing the pressure difference over the turbine, the rotational speed and the volumetric displacement (see equation 18 & 19).
- With the hydraulic losses known, the next step is to find the mechanical losses. Setting valve V_1 in a set of different positions, the turbine can be tested at a combination of different rotational speeds and pressure differences. By measuring at different rotational speeds and pressures, the torque losses that are proportional to rotational speed can be separated from the torque losses that are proportional to pressure difference by using equation 20.

Since the turbine is bi-directional, the test will be repeated in the exact same way, but with in- and outlet switched. By doing this, the efficiency of flow dependency can be found.

3. Conclusions

Within the framework of the EU H2020 funded WETFEET project, a set of breakthrough technologies have been identified to address the obstacles that have been delaying the path towards commercialization of the wave energy sector.

Efficient and robust PTO technologies is one of the obstacles to overcome. For the Symphony WEC a new efficient PTO has been designed. The PTO works in combination with a structural membrane but could also be included in other devices producing an internal flow of working fluids.

The turbine efficiency curves are determined and the maximum efficiency of the turbine is 98,5%. Applying these turbine curves in the available time domain model, for each sea state an overall conversion can be calculated.

For the representative and much occurring sea state of $T_e=10,5s$; $H_s=4,5m$ the internal conversion from hydraulic input to electrical output is 89%. Final bench tests have to confirm the efficiency curves of the turbine.

BIBLIOGRAPHY

- [1] I. Sfikas, "Evaluation and optimization of the control system of the Symphony wave power device", master thesis, 2018
- [2] D. Wikkerink, "Generator design for the Symphony wave power device", master thesis, 2017
- [3] N. Leijtens, "Optimal buffer design for the Symphony wave power system", master thesis, 2016
- [4] J. de Jong, "Design of the power take off turbine for the Symphony wave energy converter", master thesis, 2015
- [5] WETFEET Deliverable D4.2, Physical model of the selected PTO for the Symphony
- [6] WETFEET Deliverable D2.2, Report with designs and specifications of a Symphony able to integrate the control cocoon, electro-mechanic PTO, structural membrane and dielectric generators